Utilization of Third-stage waste from a Rice Production for Removal of H_2S, NO_2 and SO_2 from Air†

Teresa J. Bandosz[1,*], Rosario Ardesi[1,2], Alberto Bosio[2], Alessandra Gianoncelli[2] and Laura Depero[2] *(1) Department of Chemistry, The City College of New York, 160 Convent Avenue, New York, NY 10031, U.S.A. (2) INSTM and Chemistry for Technologies Laboratory, University of Brescia via Branze, 38, 25123 Brescia, Italy.*

(Received 2 December 2012; accepted 13 January 2013)

ABSTRACT: Materials derived from rice husk fly ash were tested as adsorbents of hydrogen sulphide, sulphur dioxide and nitrogen dioxide. Breakthrough experiments were carried out at ambient temperature either in dry or moist air. The second-stage waste obtained in the extraction of silica from fly ash using sodium hydroxide exhibits the better adsorption capacity compared with that of caustic-modified activated carbons. The high performance is related to the presence of residual sodium hydroxide and other metals such as calcium, which react with acidic gases forming corresponding salts. Moreover, a high dispersion of the alkali and alkaline earth metal sites in the mesopores renders the pH of the solution basic, aiding in the dissociation of hydrogen sulphide, thereby facilitating its oxidation. The oxidation of species is also catalyzed by the carbonaceous surface. While in the case of hydrogen sulphide and sulphur dioxide, water helps in acid–base reactions, the opposite effect is found for NO_2. Because its reactivity with water is limited, reactive metal species present in small pores are likely screened by water adsorbed at pore entrances, and therefore the adsorption of NO_2 on the surface is limited.

INTRODUCTION

Wastes, when cannot be recycled, are often considered as an alternative resource of energy. There is also a great interest in the utilization of wastes as source of valuable materials (Alexandre-Franco *et al*. 2011; Ren *et al*. 2012; Balsamo *et al*. 2013; Ioannou and Simitzis 2013). By-product materials of the combustion process can be used as a second-hand material in their original or processed forms. Relevant resources of waste originate from an agricultural sector and, in particular, from the production of rice. Rice is the second largest cereal product in the world and Italy is one of the most important producers of rice among the European nations (www.irri.org/statistics). Rice contains approximately 20% of rice husk, which consists of fibrous parts and silica-based materials. Its composition depends on the climate and the geographic location of the rice harvest (Yalcin and Sevinc 2001; Chandrasekhar *et al*. 2005). Rice husk is used as energy source and the ash generated by this process is called rice husk ash (RHA). RHA contains up to 60% of silica in the amorphous form, depending on the combustion process, and thus it can be considered a new source of silica sol or colloidal silica. Because silica-based materials are used in many applications, such as refractories, inorganic binders for paints, coating reagents with reinforcement for hard, abrasive particles, absorbents and catalysts (Pivinskii 2007;

* Author to whom all correspondence should be addressed. E-mail: tbandosz@ccny.cuny.edu (T.J. Bandosz).
†Published in the Festschrift of the journal dedicated to Professor K.S.W. Sing to celebrate his 65 years of research in the field of adsorption.

Bontempi *et al*. 2010), processes using RHA as a silica precursor have been proposed (de Sousa *et al*. 2009). The removal of silica from ash involves the extraction using aqueous sodium hydroxide (NaOH) in an autoclave (de Sousa *et al*. 2009).

The waste left after extraction of the silica gel (named RHAC) contains a carbonaceous material and a significant amount of the caustics used in the process. These features make it a plausible candidate to be used as an adsorbent to remove H_2S from air in water treatment plants (Bandosz *et al*. 2000), as a separation media in desulphurization of natural or digester gas (Seredych and Bandosz 2007) and in all the applications where activated carbons impregnated with caustics (NaOH or KOH) are applied (Bandosz 2005).

The objective of the research presented in this paper is to evaluate RHAC as an adsorbent of H_2S, NO_2 and SO_2 from air. The performance in dynamic conditions is linked to surface chemical and physical properties. The detailed characterization of this material surface and indication of its suitability towards specific environmental applications can throw a new light on fly ash waste utilization.

EXPERIMENTAL SETUP

Materials

The RHA sample was obtained from industrial combustion of rice husk. The process was carried out at temperature of approximately 900 °C. The sample was digested with aqueous NaOH (1 M solution) for approximately 1 hour at 100 °C. Approximately 100 g of RHA was treated with 1 l of NaOH solution. Then silica gel was separated by filtration, followed by washing (de Sousa *et al*. 2009). The residue obtained in this process, which amounts to approximately 95%, was dried at 100 °C and is referred as RHAC. The exhausted samples after adsorption runs in dry conditions have the letter D added to their names, and in moist conditions the letter M. The challenge gas is referred to by its chemical formula. Thus, for example, RHAC-M-H_2S refers to the exhausted sample RHAC run in moist conditions as an H_2S adsorbent.

Methods

H_2S, SO_2 and NO_2 breakthrough capacity

Dry or moist (70% humidity) air, containing 0.1% H_2S, SO_2 or NO_2 (1000 ppm), was passed through a column (length 370 mm, diameter 9 mm) with 2 cm^3 of either RHA or RHAC mixed with glass beads (the volume ratio of the sample to glass beads was 20%). The flow rate was 0.25 l/minute and the experiments were carried out at room temperature. The H_2S and SO_2 concentration were measured by an Interscan LD-17 continuous monitor system (electrochemical detector). The tests were stopped at a breakthrough concentration of 100 ppm (detector limit). The NO_2 concentration was measured using a RAE Multiscan gas monitor and the tests were stopped at 250 ppm. The breakthrough capacity of adsorbents for the particular gas in dry (D) or moist (M) conditions was then calculated using the integrated area above the breakthrough curve, the mass of the adsorbent and the flow rate. The following equation was used to calculate the adsorption capacity:

$$Q_m = Q_n + \left[\frac{\left\{ \left[500 - \left(\frac{c_n + c_m}{2} \right) \right] \times \left(t_m - t_n \right) \times F_{tot} \times MW \times 273 \right\}}{\left[10^6 \times w_t \times 22.4 \times 273 + T_C \right]} \right]$$

where Q_m is the capacity after time t_m, Q_n the capacity after time t_n, C_n the detected concentration after time t_n, C_m the concentration after time t_m, F_{tot} a total flow rate, MW is the molecular mass of the adsorbate, w_t is the weight of the carbon bed and T_c is the temperature of measurement in °C. The presence of weakly adsorbed H_2S/SO_2 gas was monitored by purging the column with air.

Surface area and porosity evaluation

Nitrogen adsorption isotherms were measured using an ASAP 2020 analyzer (Micromeritics, Norcross, GA, U.S.A.) at –196 °C. Before the experiment, the samples were degassed at 120 °C to a constant pressure of 10^{-4} Torr. The isotherms were used to calculate the specific surface area, S_{BET}; micropore volume, V_{mic}; total pore volume, V_t (calculated from the amount of N_2 adsorbed at $p/p_0 = 0.98$); and pore-size distributions (PSDs). The micropore volume was calculated using Dubinin–Radushkevich approach (Dubinin 1966) and the total pore volume was obtained from the volume of nitrogen adsorbed at the last point of the isotherm. The volume of mesopores, V_{mes}, represents the difference between those two values. The relative microporosity was calculated as the ratio of the micropore volume to the total pore volume. PSDs were calculated using the density functional theory method (Lastoskie *et al*. 1993).

pH of the surface

A 0.1 g sample of dry adsorbent was added to 5 ml of deionized water and the suspension was stirred overnight to reach equilibrium. The sample was filtered and the pH of solution was measured using an Accumet Basic pH meter (Fisher Scientific, Springfield, NJ, U.S.A.).

Thermal analysis

Thermal analysis was carried out using a Thermal Analyzer (TA Instruments, New Castle, DE, U.S.A.). The heating rate was 10 °C/minute in a nitrogen atmosphere at 100 ml/minute flow rate. The samples were heated up to 1000 °C.

Total X-ray fluorescence

Total X-ray fluorescence (TXRF) measurements were performed using the Bruker TXRF system S2 PICOFOX (air cooled, Mo tube, Silicon-Drift Detector) with operating values of 50 kV and 750 mA, using an acquisition time of 600 seconds. TXRF quantitative analysis of the solution samples was performed by the internal standard procedure. A proper amount of gallium, used as an internal standard element, was added to the right sample solution volume in order to obtain a Ga concentration of 1 mg/l.

Fourier transform infrared

Fourier transform infrared spectroscopy measurements were carried out on a Nicolet Magna-IR 830 spectrometer using the attenuated total reflectance method. The spectrum was generated and collected 32 times and corrected for the background noise. The experiments were done on the powdered samples, without KBr addition.

Elemental analysis

The samples were dried in platinum crucible at 105 °C and ashed at 700 °C. Ash was ground in a mortar and about 100 mg of the sample was fluxed with $Li_2B_4O_7$ and the mixture is diluted to 0.2 l by adding 5% HCl. The analysis was done using Varian ICP.

RESULTS AND DISCUSSION

For the potential application of any material as an adsorbent, a detailed surface characterization should be carried out by addressing its porosity and surface chemistry. The latter is especially important when reactive adsorption is involved and this adsorption mechanism is indeed our target because the physical adsorption forces for our adsorbates at ambient conditions are expected to be small (Bandosz 2002; Bandosz and Petit 2009; Bandosz 2012).

The parameters of porous structure and PSDs calculated from nitrogen adsorption isotherms are presented in Table 1 and Figure 1, respectively. Even though the materials studied cannot be considered as porous media, some porosity is detected, especially in the range of mesopores. If the appropriate chemistry exists, these pores can contribute to reactive adsorption (Bandosz 2012).

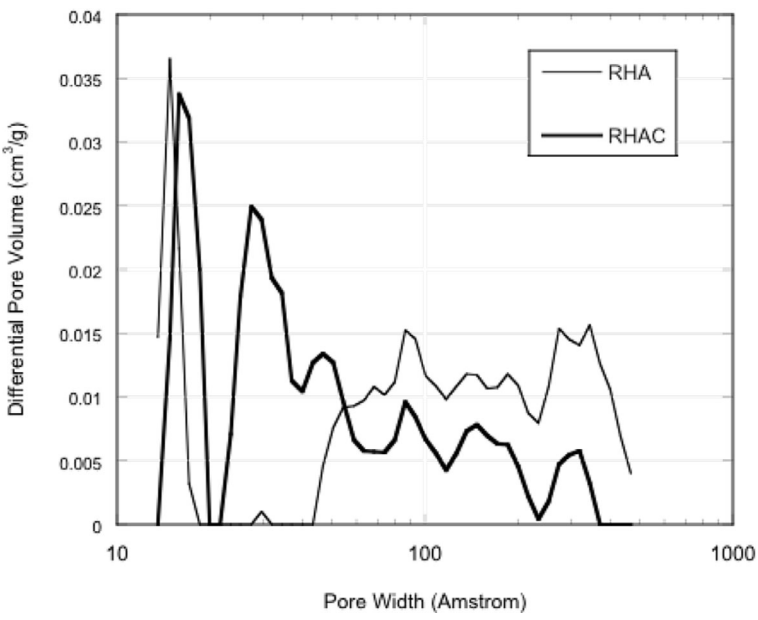

Figure 1. Pore-size distributions for the materials studied

TABLE 1. Parameters of Porous Structure Calculated from Nitrogen Adsorption Isotherms

Sample	S_{BET} (m^2/g)	V_{micDA} (cm^3/g)	V_{mes} (cm^3/g)	V_t (cm^3/g)
RHA	37	0.02	0.03	0.05
RHAC	84	0.04	0.04	0.08
RHAC-D-H2S	27	0.01	0.01	0.02
RHAC-M-H2S	16	0.01	0.01	0.02
RHAC-D-SO2	39	0.02	0.02	0.04
RHAC-M-SO2	37	0.02	0.02	0.04
RHAC-D-NO2	34	0.02	0.02	0.04
RHAC-D-NO2	46	0.02	0.03	0.05

The main difference between RHA and RHAC is the presence of mesopores in the latter material with sizes less than 30 Å. Those pores are important as physical adsorption centres and they can also work as nanoreactors when water is present in the system and it participates in reactive adsorption (Bandosz 2002).

Scanning electron microscopic images of RHA and RHAC samples are shown in Figure 2. The dramatic change in the morphology is evident as a result of silica extraction. The surface of RHA consists of large particles of a smooth surface, which is likely to be silica. After reaction with NaOH, the smaller particles appear to contain a heterogeneous surface. The detected increase in porosity must be the result of silica removal.

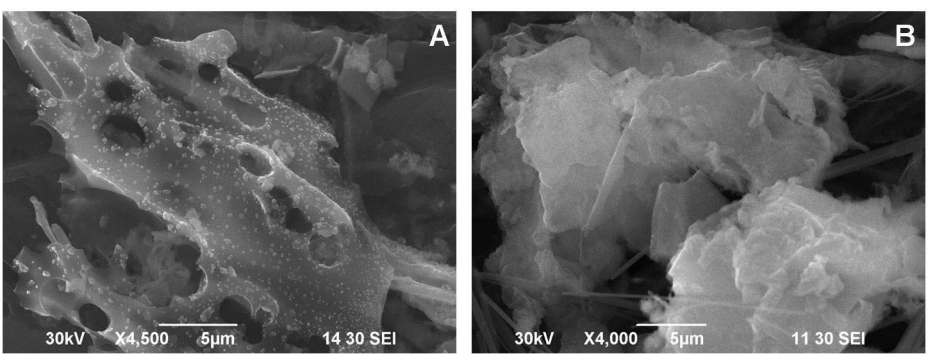

Figure 2. Scanning electron microscopic image of RHA (A) and RHAC (B)

From the point of view of surface chemistry differences exist, which are related to the nature of the materials. RHAC is obtained from RHA, and therefore its silica content is decreased 20% and is richer in the carbonaceous material originating from incomplete combustion process (Table 2). The content of carbon increased from approximately 10% to 30%. Another important feature of RHAC is the presence of a significant amount of caustic because NaOH was used as a silica extraction agent. The elemental analysis data also show the high concentration of potassium, calcium and magnesium, which can be important for reactive adsorption of acidic gases (Bandosz 2012). This might explain the basic pH (pH = 11) of the RHAC sample. Other important species, which might contribute to catalytic oxidation reactions, are iron and manganese oxides [14] present in the inorganic phase in marked quantities. The XRD patterns for RHA and RHAC samples are shown in Figure 3. As it can observed, cristobalite is the only crystalline phase

TABLE 2. Results of Elemental Analysis Obtained Using TXRF and ICP [a] Analyses

(%)	TXRF	(ppm)	ICP elements	(ppm)	Oxide	ICP
	RHA	RHAC	RHA	RHAC		RHA	RHAC
Al	ND	ND	3646	4247	Al_2O_3	0.62	0.92
Ba	ND	ND	38	57	BaO	0.00	0.01
Ca	7342	11,207	9473	18,061	CaO	1.18	2.89
Cr	ND	ND	84	109	Cr_2O_3	0.01	0.02
Cu	10	18	159	212	CuO	0.02	0.03
Fe	725	859	1125	3165	Fe_2O_3	014	0.52
K	12,430	6525	20,113	12,140	K_2O	2.16	1.67
Mg	ND	ND	2970	5511	MgO	0.44	1.04
Mn	1005	1955	2276	3499	MnO_2	0.32	0.63
Na	ND	ND	1026	88,369	Na_2O	0.12	13.62
Ni	10	6	63	108	NiO	0.01	0.02
Si	104,808	81,857	496,724	320,968	SiO_2	94.93	78.52
Ti	30	50	62	187	TiO_2	0.01	0.04
Zn	115	180	247	561	ZnO	0.03	0.08
Carbon phase [b]	ND	ND	9.69	29.13	–	–	–

a Analysis of ash.
b Based on the burning at 700 °C.

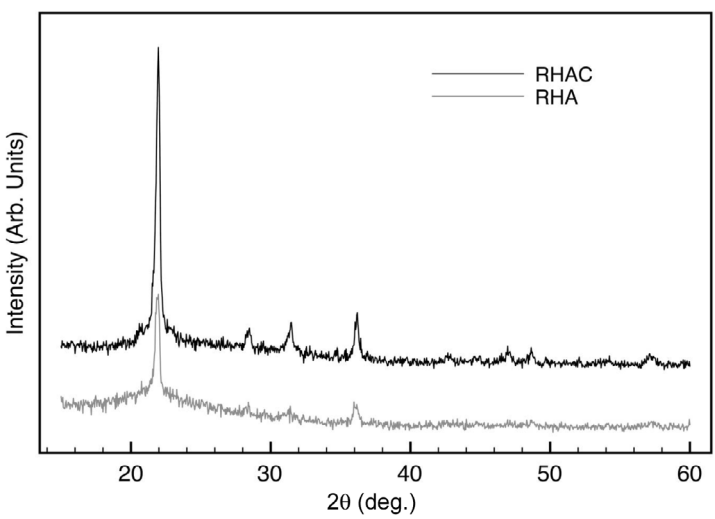

Figure 3. Comparison of X-Ray diffraction patterns for the RHA and RHAC samples.

detected. The amount of amorphous silica significantly decreased in the RHAC sample while the cristobalite phase is still present.

The comparison of the H_2S, SO_2 and NO_2 breakthrough curves for RHAC run in moist and dry conditions is presented in Figure 4. The calculated capacities are collected in Figure 5. They are

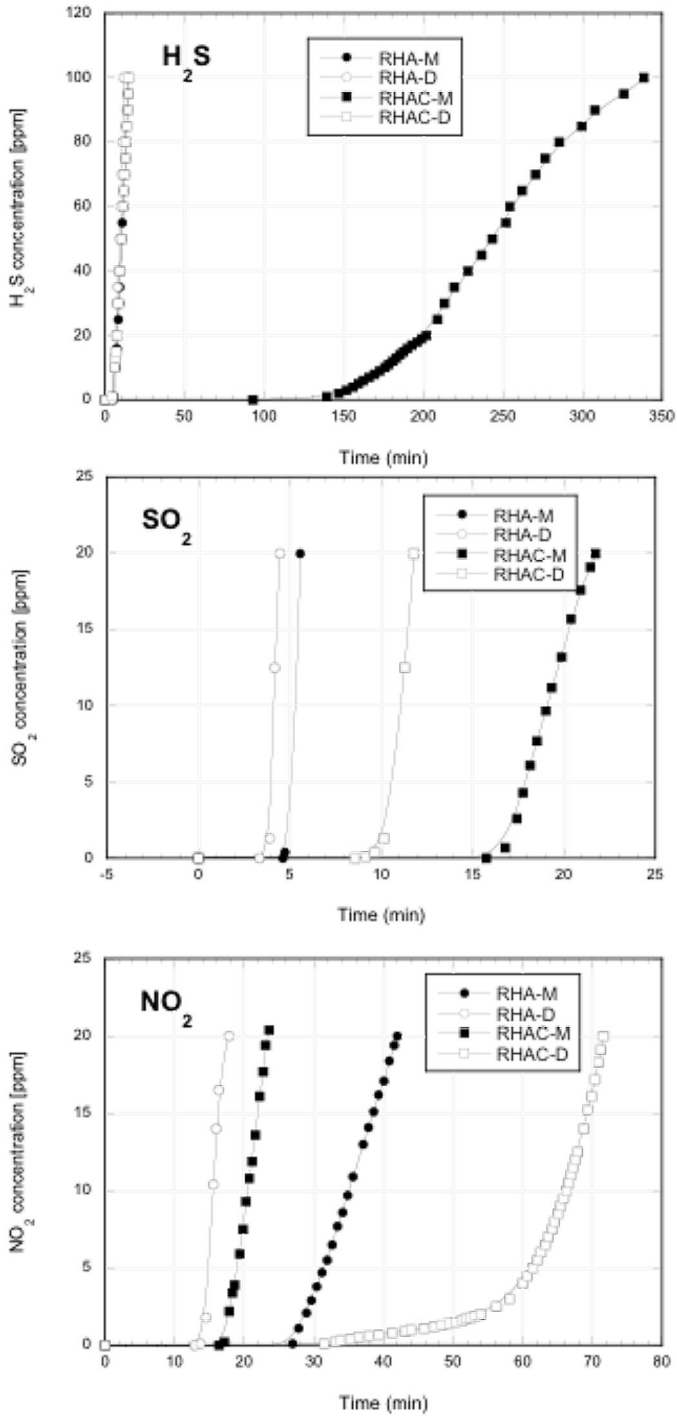

Figure 4. Breakthrough curves for the target gases on RHAC measured in moist (M) and dry (D) conditions.

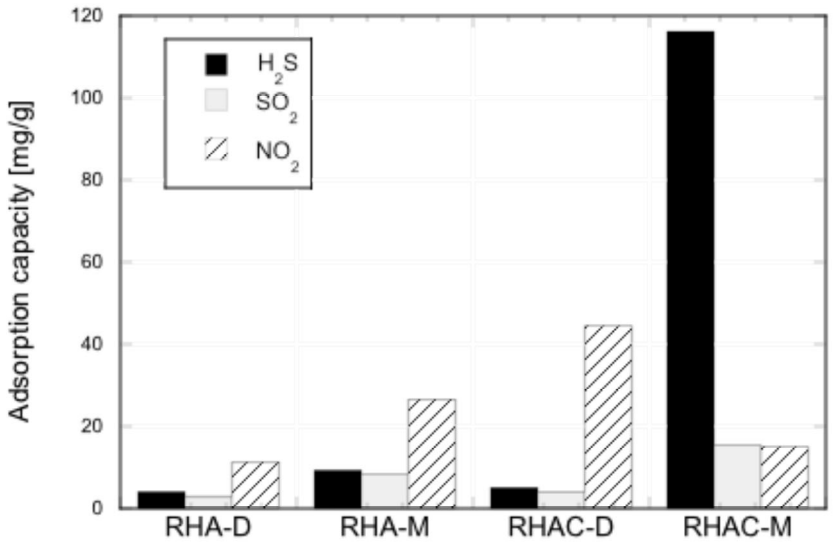

Figure 5. Comparison of the measured breakthrough capacities for toxic gases.

comparable to those measured on modified activated carbons, which were reported to be approximately 150, 75 and 130 mg/g for H_2S, SO_2 and NO_2 removal, respectively (Bandosz 2005). These ranges of capacities were measured at the same conditions as those used for the estimating the performance of the RHAC sample. The breakthrough times for all gases measured on RHA were negligible in comparison with those measured on RHAC. The presence of moisture visibly increases the performance for H_2S and SO_2 adsorption and this is in agreement with other studies (Bandosz 2002). The shape of the breakthrough curves also changes and less steepness in moist conditions suggests that chemical reactions take place on the surface. Water is likely involved in this process. Interestingly, for NO_2, the breakthrough time is longer in dry conditions than that in moist gas. The RHAC sample appears to be the most suitable adsorbent for hydrogen sulphide removal.

To evaluate the role of surface features, a detailed analysis of the exhausted samples was carried out. Because the performance of RHA is rather poor and cannot be considered as a good adsorbent, all analysis were on done on RHAC samples exhausted in the dry and wet runs. The porosity data are collected in Table 1. Even though the differences in the porosity exist, the samples can be considered as rather non-porous and this is an indication that surface chemistry is a predominant factor affecting the adsorptive performance. A measured decrease in the surface areas ranges from 30% to 80%. The latter is measured on the RHAC exposed to H_2S in moist conditions where approximately 12% wt. of hydrogen sulphide was adsorbed. Interestingly, the decrease does not follow the amount adsorbed and the adsorbents after NO_2 removal exhibit the least pronounced changes in porosity. It is possible that nitrates or nitrates are formed in reactions with sodium, and other reactive metals or the carbon phase decompose during the high vacuum heating at 120 °C (Weast and Astle 1982). Sulphites/sulphates and sulphides/sulphur are much more thermally stable.

To analyze the deposition of surface reaction products, the PSDs were calculated from nitrogen adsorption isotherms for the exhausted samples (Figure 6). For comparison, the PSDs for the initial sample are also included in Figure 6. While in the case of H_2S adsorption, pores smaller

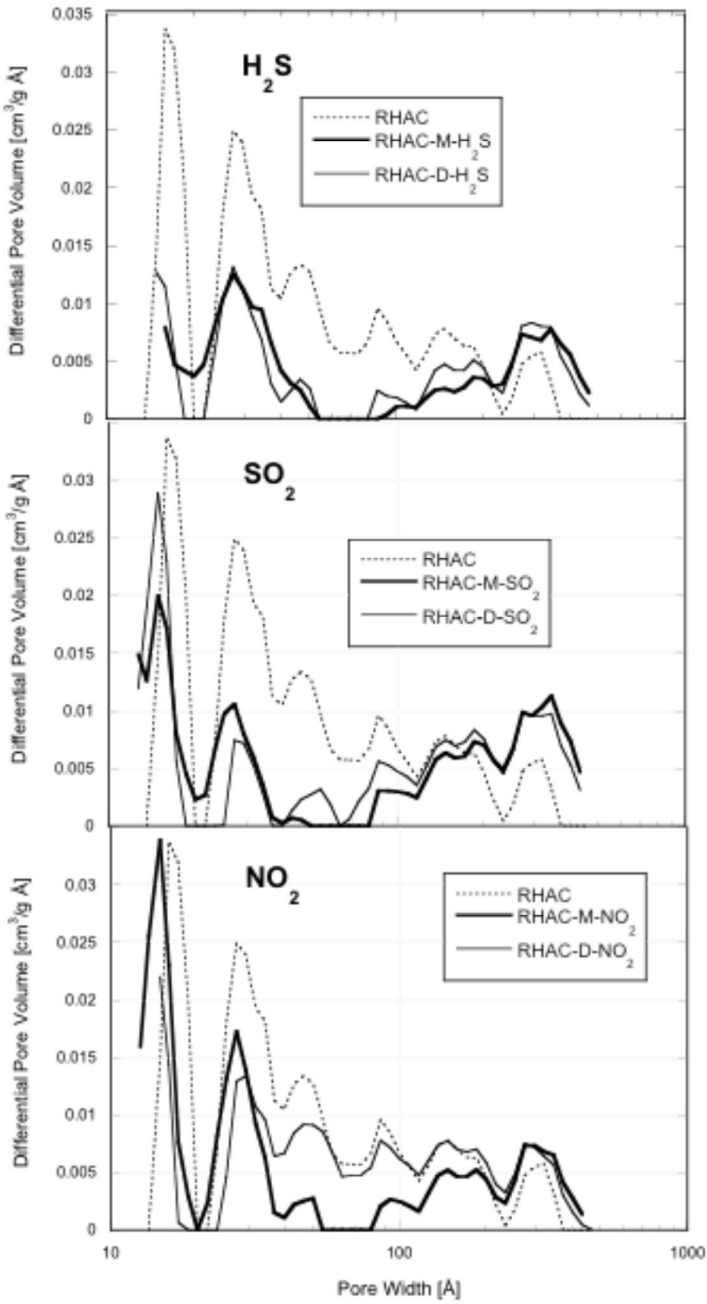

Figure 6. Comparison of pore-size distributions for the initials and exhausted RHAC samples exposed to target gases at moist (M) and dry (D) conditions.

than 100 Å are occupied by the surface reaction products, in the case of the SO_2 adsorption, the pores between 20 and 100 Å seem to be active and an increase in the volume of large pores, bigger than 200 Å, is observed. Interestingly, there are not marked differences in PSDs for the samples run in dry and wet conditions, even though in the case of H_2S a large difference in the capacity is found. The changes in the porosity of the material after NO_2 adsorption show the main involvement of pores between 30 and 100 Å with marked differences in the distributions depending on the conditions of the experiments. Even though the capacity in dry conditions was higher than that in the moist ones, the changes in PSD do not reflect that trend. The plausible explanation is the decomposition of weakly adsorbed NO_2 in dry conditions. In fact, the formation of nitric acid being able to be deposited as nitrates is not expected in this case (Pietrzak and Bandosz 2008).

To further analyze the surface reaction products and provide more information needed to derive the mechanism of adsorption, thermal analysis was run in nitrogen on the exhausted and initial samples. The results are compared in Figure 7. The peaks represent weight loss related to the decomposition or removal of specific chemical compounds from the materials' surface. Even though the adsorbents change during this analysis, a comparison of the initial and exhausted samples can provide valuable information about the changes in surface chemistry caused by reactive adsorption (Bandosz 2002; Bandosz and Petit 2009; Bandosz 2012). The results are analyzed taking into account that sodium and calcium are the main reactive metals present in the samples.

After H_2S adsorption in moist conditions, significant changes in the weight loss pattern are found compared with the initial sample. The first peak at approximately 100 °C represents removal of water by the physically/weakly adsorbed hydrogen sulphide. Then the complex and continuous weight loss pattern between 100 and 450 °C is assigned to the decomposition of Na_2SO_3 (approximately 150 °C), Na_xS_y (250–300 °C), $NaHSO_4$ (315 °C), NaHS (350 °C), $Na_2S_2O_7$/elemental sulphur (400 °C) (Weast and Astle 1982). A broad peak between 600 and 800 °C is linked to the decomposition of Na_2SO_4. These results indicate that besides acid–base reactions, oxidation of hydrogen sulphide takes place. These reactions are expected in the presence of water and air in the basic environment. This mechanism of surface interactions was described in detail by Bagreev and Bandosz (2002). The intense peak centred at 700 °C on the curve for the sample run in moist conditions indicates that water is necessary for the formation of sulphuric acid and thus sulphates. In the case of sample run in dry conditions, only water in equilibrium with the atmosphere was present on the surface, and therefore the peak representing decomposition of sulphates is much less intense. Other well-visible peaks represent removal of weakly adsorbed SO_2 at 80 °C, decomposition of sodium sulphite (150 °C) and Na_xS_y (220–300 °C) (Weast and Astle 1982).

After SO_2 adsorption in moist conditions, a predominant peak representing the decomposition of sodium sulphate is present. This peak has very similar intensity to the one detected on the derivative thermogravimetric (DTG) curve after H_2S adsorption in moist conditions. This suggests that the amount of sodium sulphate formed during H_2S adsorption is governed by the amount of sodium. The intensity of that peak in dry conditions is also similar to that found on the exhausted sample after H_2S adsorption. DTG curves suggest that when SO_2 is adsorbed in the absence of moisture more Na_2SO_3 and $NaHSO_4$ are formed than when the experiment is run in most conditions. In the latter experiment, these species must react further to form sodium sulphate.

The DTG curve for the sample exposed to NO_2 in dry conditions exhibit the peaks at approximately 100, 200 and 400 °C. They are assigned to the removal of weakly adsorbed NO_2, sodium nitrite and sodium nitrate, respectively (Weast and Astle 1982). The most pronounced is

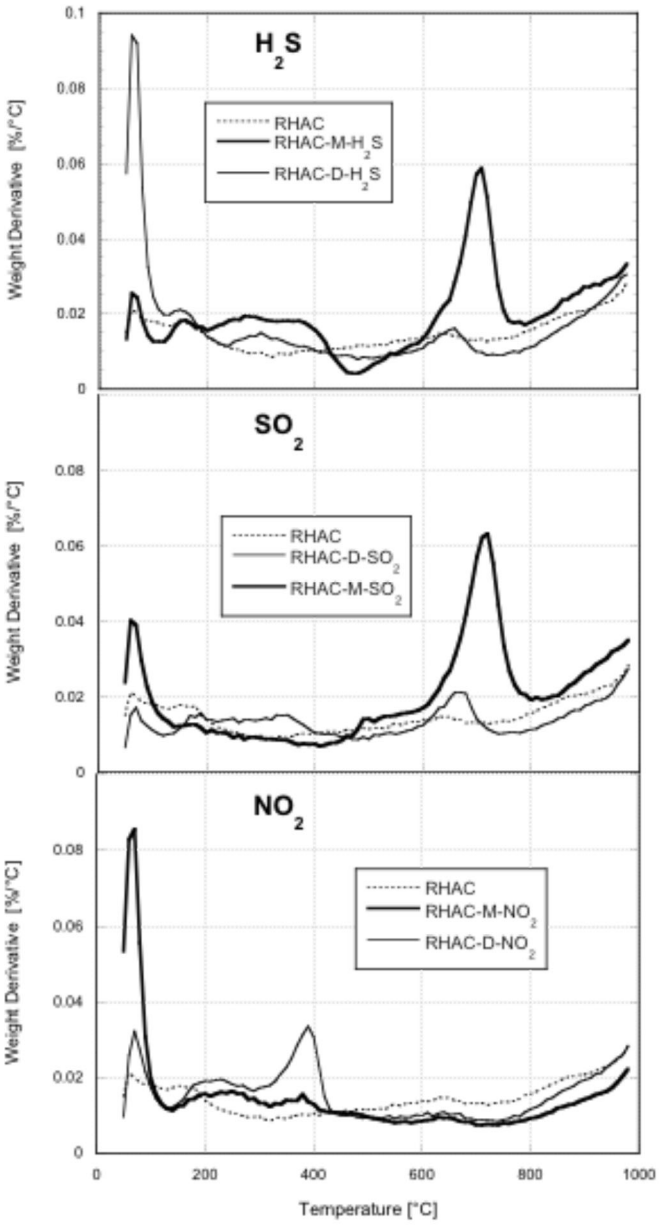

Figure 7. Comparison of DTG curves measured in nitrogen for the initials and exhausted RHAC samples exposed to target gases at moist (M) and dry (D) conditions.

the nitrate peak. This species decomposes at 380 °C. Its appearance is a proof of the oxidation reactions taking place on the surface. After adsorption in moist conditions, only small amounts of nitrite and nitrate are detected but the intensity of the first peak significantly increases. This peak might represent the removal of water. These results suggest that water blocks NO_2 adsorption centres. It is likely that it adsorbs at the mouth of small pores on the hydrophilic centres related to the inorganic mater/silica, thus making the majority of sodium centres inaccessible for reactions with NO_2.

Changes in surface chemistry imposed by reactive adsorption of our target gases were also evaluated using infrared spectroscopy. The spectra are presented in Figure 8). After H_2S adsorption, the intensities of the bands at 1450 cm^{-1} increase for the samples run in dry and wet conditions. It is linked to the presence of organic sulphates formed in the reactions of sulphuric acid with the carbon phase (Miller and Wilkins 1952; Trenter *et al*. 2000). Moreover, in the case of the latter sample, the new bands at 890 and 820 cm^{-1} appear. They are assigned to the vibrations of sodium bisulphate (Miller and Wilkins 1952; Trenter *et al*. 2000). The detection of sulphides using this method is not expected owing to the low intensity of the vibrations. The main bands visible for all samples at 800 and 1100 cm^{-1} represent Si–O–Si bonds. After SO_2 adsorption, the intensity of the band at 1450 cm^{-1} related to the presence sodium sulphate (Miller and Wilkins 1952) increases. Small changes in the ranges of sulphite vibration at about 600 cm^{-1} are also noticed. The exposure to NO_2 in moist and dry conditions results in distinctively different spectra. In dry conditions, the split band at about 1400 cm^{-1} appears and it is linked to the presence of nitrate ions (Goebbert *et al*. 2009). In moist conditions, the band at 1450 cm^{-1} visibly increases its intensity and the band at about 900 cm^{-1} appears. The shift of the band at about 1400 cm^{-1} to a higher wave number indicates the hydration of nitrates owing to the presence of water in the system (Goebbert *et al*. 2009). Sodium nitrites and nitrates are expected to show vibration at about 840 cm^{-1}.

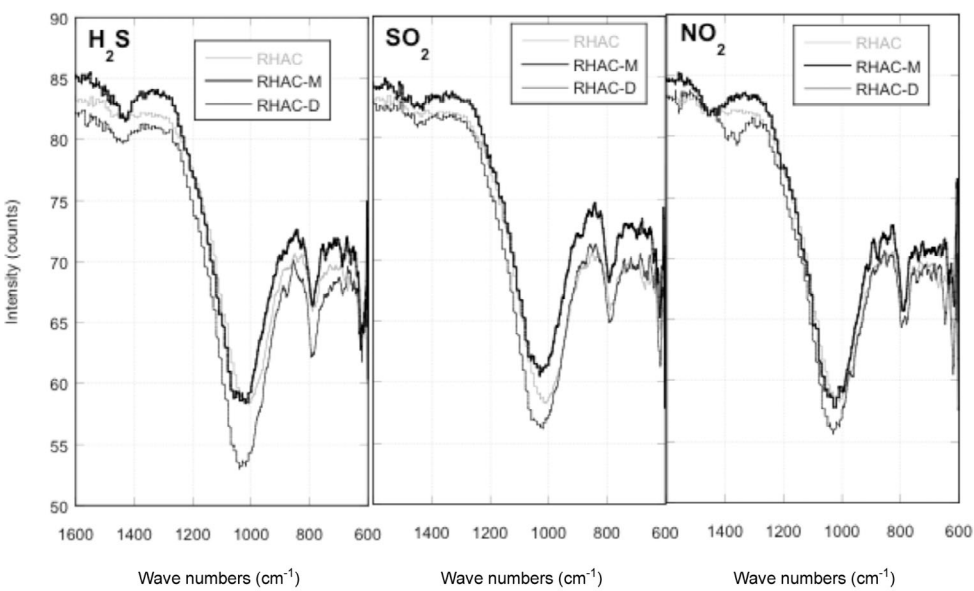

Figure 8. Comparison of Fourier transform infrared spectra for the initials and exhausted RHAC samples exposed to target gases at moist (M) and dry (D) conditions.

Based on the discussion of the results presented in the previous sections, the high capacity of the RHAC sample cannot be exclusively linked to its developed mesoporosity, although the small pores likely between the carbonaceous particles of the fly ash constituents should attract the molecules of gases via physical adsorption. In fact, the presence of residual sodium hydroxide on the surface of this material seems to be of paramount importance for the reactive adsorption. In the presence of caustics, the mechanism of H_2S reactive adsorption should follow the one presented elsewhere (Bagreev and Bandosz 2002). Thus, sodium hydroxide besides directly reacting with hydrogen sulphide provides basic pH for H_2S dissociation and formation of HS^-. Those ions are oxidized by air to various oxysulphur species and thus sulphates are formed (Bashkova *et al*. 2001; Bandosz 2002). Because sodium is the predominant reactive cation, its salts are detected on the surface. In the case of sulphur dioxide adsorption, sulphates are formed in a direct reaction with NaOH or calcium oxides and they undergo oxidation to form sulphates (Bandosz 2002). Iron and manganese species likely facilitate this process (Bashkova *et al*. 2001). The carbon phase present in the RHAC adsorbent can also contribute to the activation of oxygen formation of superoxide ions and thus an increase in the extent of oxidation reactions (Stohr and Boehm 1991). Water is an important factor for these reactions because it helps in the dissociation of the species and acid–base reactions.

The interactions of NO_2 with the surface follow a different scenario. Even though sodium or calcium nitrites can be formed during the direct reaction of sodium hydroxides and nitrogen dioxide (Lee *et al*. 2002), the presence of water has a detrimental effect on the NO_2 retention. This can be explained by adsorption of water at the entrance to the pores where sodium hydroxide exists. This process screens the reactive centres and thus limits their accessibility for adsorbate molecules. In contrast to the behaviour of H_2S or SO_2, water does not directly increase the reactivity of NO_2 by forming an acid, which could undergo an acid–base reaction with sodium hydroxide. An additional reaction taking place on the surface is oxidation of nitrite to nitrates (Pietrzak and Bandosz 2008) and it is facilitated by iron/manganese species and the catalytic carbon phase.

CONCLUSIONS

The results presented in this paper show the possibility of utilization of the third-stage waste derived from biomass as efficient adsorbents of toxic acidic gases. Its suitability for reactive adsorption is linked to the carbon phase and to the presence of residual alkali and alkaline earth metals left in the materials after the removal of colloidal silica. The carbon phase, besides providing the surface for the high dispersion of reactive sodium hydroxide, also catalyses oxidation through the formation of the superoxygen ions. Iron and manganese species also contribute to these reactions. Sodium hydroxide is the main reactive species binding the acidic gases in the form of salts. The adsorbents show the capacity for the removal of toxic acidic gases similar to that obtained on modified activated carbons.

Acknowledgement

T.J.B. is grateful to Mr. Albert Tamashausky of Asbury Carbon for his help with the ICP analysis.

REFERENCES

Alexandre-Franco, M., Fernández-González, C., Alfaro-Domínguez, M. and Gómez-Serrano, V. (2011) *J. Environ. Manage*. **92**, 2193.
Bagreev, A. and Bandosz, T.J. (2002) *Ind. Eng. Chem. Res*. **41**, 672.
Balsamo, M., Di Natale, F., Erto, A., Lancia, A., Montagnaro, F. and Santoro, L. (2013) *Fuel* (in press).
Bandosz, T.J. (2002) *J. Colloid Interf. Sci*. **246**, 1.
Bandosz, T.J. (2005) *Adsorption by Carbons*, E.J. Bottani and J.M.D. Tascon, editors. Elsevier, Amsterdam.
Bandosz, T.J. (2012) *Catal. Today* **186**, 20.
Bandosz, T.J., Bagreev, A., Adib. F. and Turk A. (2000) *Environ. Sci. Tech*. **34**, 1069.
Bashkova, S., Bagreev, A., Locke, D.C. and Bandosz, T.J. (2001) *Environ. Sci. Technol*. **35**, 3263.
Bandosz, T.J. and Petit, C. (2009) *J. Colloid Interf. Sci*. **338**, 329.
Bontempi, E., Zacco, A., Borgese, L., Gianoncelli, A., Ardesi, R. and Depero, L.E. (2010) *J. Environ. Monit*. **12**, 2093
Chandrasekhar, S., Pramada, P.N. and Praveen, L. (2005) *J. Mater. Sci*. **40**, 6535.
de Sousa, A.M., Visconte, L., Mansur, C. and Furtado, C. (2009) *J. Chem. Technol*, **3**, 69.
Dubinin, M.M. (1966) Porous structure and adsorption properties of active carbons. In: *Chemistry and Physics of Carbon*. Marcel Dekker, New York, p. 51.
Goebbert, D.J., Garand, E., Wende, T., Bergmann, R., Meijer, G., Asmis, K.R. and Neumark, D.M. (2009) *J. Phys. Chem. A* **113**, 7584
Ioannou, Z. and Simitzis, J. (2013) *Bioresour. Technol*. **129**, 191.
Lastoskie, C.M., Gubbins, K.E. and Quirke, N. (1993) *J. Phys. Chem*. **97**, 4786.
Lee, Y.W., Park, J. W. and Hun, J. H. (2002) *Environ. Sci. Technol*. **36**, 4928
Miller, F.A. and Wilkins, C.H. (1952) *Anal. Chem*. **24**, 1253.
Pietrzak, R. and Bandosz, T.J. (2008) *J. Hazard. Mater.* **154,** 946.
Pivinskii, Y. (2007) *Refract. Ind. Ceram*. **48**, 408.
Ren, X., Liang, B., Liu, M., Xu, X. and Cui, M. (2012) *Bioresour. Technol*. **125**, 300.
Seredych, M. and Bandosz, T.J. (2007) *Energy Fuels* **21**, 858.
Stohr, B. and Boehm, H.P.(1991) *Carbon* **29**,707.
Trenter, G., Holmes, J. and Lindon, J. (2000) *Encyclopedia of Spectroscopy and Spectrometry*. Academic Press, New York.
Weast R.C. and Astle M.J. (1982) *Handbook of Chemistry and Physics*. CRC Press, Boca Raton, FL.
Yalcin, N. and Sevinc, V. (2001) *Ceram. Int*. **27**, 219.